

Gabriela A. N. Crespi,^a David B. Ascher,^a Michael W. Parker^{a,b} and Luke A. Miles^{a,b*}

^aACRF Rational Drug Discovery Centre and Biota Structural Biology Laboratory, St Vincent's Institute of Medical Research, 9 Princes Street, Fitzroy, Victoria 3056, Australia, and ^bDepartment of Biochemistry and Molecular Biology, Bio21 Molecular Science and Biotechnology Institute, University of Melbourne, Parkville, Victoria 3010, Australia

Correspondence e-mail: lmiles@svi.edu.au

Received 5 December 2013

Accepted 22 January 2014

Crystallization and preliminary X-ray diffraction analysis of the Fab portion of the Alzheimer's disease immunotherapy candidate bapineuzumab complexed with amyloid- β

Bapineuzumab (AAB-001) and its derivative (AAB-003) are humanized versions of the anti-A β murine antibody 3D6 and are immunotherapy candidates in Alzheimer's disease. The common Fab fragment of these immunotherapies has been expressed, purified and crystallized in complex with β -amyloid peptides (residues 1–8 and 1–28). Diffraction data at high resolution were acquired from crystals of Fab–A β_8 (2.0 Å) and Fab–A β_{28} (2.2 Å) complexes at the Australian Synchrotron. Both crystal forms belonged to the primitive orthorhombic space group $P2_122_1$.

1. Introduction

Alzheimer's disease (AD) is a progressive, age-related neurodegenerative disorder and is amongst the leading causes of death in the developed world. Over 35 million people worldwide currently live with AD and this is expected to reach 115 million by 2050 according to the World Alzheimer's Report 2013 (Prince *et al.*, 2013). Currently there is no cure for AD (Selkoe, 2012). The neuropathology of AD is characterized by the presence of neurofibrillar tangles and extracellular senile plaques (Selkoe, 1999). Neurofibrillary tangles consist of hyperphosphorylated tau protein that adopts a double-helical filament conformation. The major component of the senile plaques is aggregates of a 4 kDa peptide called amyloid- β or A β (Masters *et al.*, 1985). The A β peptide is the product of sequential cleavage of the membrane-bound amyloid precursor protein (APP) by β -site APP-cleaving enzyme (BACE) and the integral membrane protein complex γ -secretase (Tabaton & Tamagno, 2007). These peptides can self-associate and adopt several neurotoxic forms. Therefore, A β is thought to play a crucial role in the pathogenesis of AD. Consequently, many therapeutic approaches to inhibit A β production, aggregation and clearance from the brain are currently being trialled.

Immunotherapy targeting of A β is one of the strategies being pursued. Active immunization with the A β peptide triggers the production of antibodies that can prevent and clear amyloid in transgenic AD mice and improve or prevent behavioural deficits (Chen *et al.*, 2007). Clinical trials to evaluate the safety and efficacy of the AN1792 vaccine (pre-aggregated A β immunogen; Gilman *et al.*, 2005) were abandoned owing to 6% of the participants developing sterile meningoencephalitis (Orgogozo *et al.*, 2003). This was thought to be a T-cell-mediated response (mid- and C-terminal epitopes), and subsequent active immunogens being developed were restricted to the A β amino-terminal region, the immunodominant B-cell epitope of A β .

Passive immunotherapies (administration of anti-A β antibodies) have been developed targeting N-terminal, mid- and C-terminal regions of A β . Bapineuzumab is the most comprehensively trialled immunotherapy to treat AD in the clinic. It is a humanized antibody from the parent murine IgG monoclonal antibody 3D6 and is specific for the N-terminal five amino acids of A β (Johnson-Wood *et al.*, 1997). Bapineuzumab is the only drug clinically proven to prevent accumulation of A β in the brain of patients with mild to moderate AD (Rinne *et al.*, 2010) and lowers phosphorylated tau protein in cerebrospinal fluid (CSF; Blennow *et al.*, 2012). Unfortunately, it failed to improve cognitive and functional decline in mild to moderate AD sufferers and was toxic at higher doses (<http://www.alzforum.org/new/detail.asp?id=3268>). An Fc-modified form of



Table 1
Humanized 3D6 Fab chain sequences.

Light chain	MESQTQVLM SLLFVWSGTCGYVVM TQSP LSLPVTPGEPASIS-CKSSQSL LDSDGKTYLNWLLQKPGQSPQRLIYL VSKLDSGVPDRFSGSGS GTDFTLKISRVEAEDVGYVYC WQGT HFPRTFGQGT KVEIKRTVAAPSVF IFPPSDEQLKSGTASV VCLLN NYFPREAKVQWKVDNALQSGNSQESVTEQDSK DSTYLSSTLTL SKADYEKHKVYACEVTHQGLSSPVTKSF NRGEC
Heavy chain	MGWSWIFLFLVSGTGGV LSEVQLLES GGGLVQPGGSLRL SCAAS GF TFSNYGMSWVRQAPG KGLEWVASIRSGG RTYYSDNVKGRFTISRDNA NSLYLQMN SLRAEDTALYCVRYD HYS GSDDYWGQGT LVTVSSASTK GPSVF PLAPSSK STSGGTAALGCLVKDYF PPQVTVSWNSG ALTS GVHTFPAVLQSSGLY SLSSV TV PS SLGTQTYICNVNHKPSNTK VDKK VEPKSCH HHHHH

bapineuzumab, AAB-003, which is expected to have a better safety profile, is in clinical trials and is a potential preventative treatment for AD (Moreth *et al.*, 2013).

We have previously determined the molecular basis of the recognition of A β of another N-terminal-specific antibody (Miles *et al.*, 2008). The WO2 antibody recognized the N-terminal A β residues 2–8 in an extended conformation. It was thus intriguing to explore whether bapineuzumab would recognize the N-terminal region of A β in the same way. Here, we report the details of our strategy to express, purify and crystallize the Fab of bapineuzumab in complex with A β in order to understand the action of the clinically important AD immunotherapy.

2. Experimental procedures and results

Initially, we expressed intact humanized monoclonal 3D6 antibody constructs for crystallization trials. Our first attempts yielded crystals and structures for the Fc portion only, formed ‘in-drop’ by proteolytic breakdown. Attempts to obtain Fab fragments by traditional Mab digestion of the intact antibodies (Wun *et al.*, 2008) yielded very small amounts of protein. To overcome these limitations, we co-expressed different light-chain and heavy-chain constructs for humanized 3D6 Fabs. The first construct to yield diffracting crystals was Fab expressed with a C-terminal hexa-His-tagged heavy chain.

2.1. Expression and purification

We obtained synthetic DNA cloned into pcDNA3.1 expression vectors from GenScript for expression of the heavy and light chains.

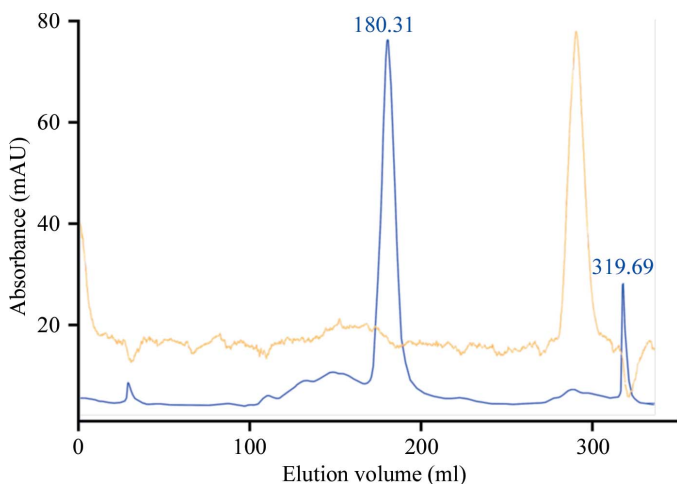


Figure 1
Purification of the Fab from bapineuzumab by size-exclusion chromatography. The blue trace is absorbance at 280 nm and the yellow trace represents conductivity.

Sequences were reconstructed from published amino-acid sequences (Schroeter & Games, 2008). The N-terminal signal peptides were incorporated for the heavy chain (MGWSWIFLFLVSGTGGVLSE) and light chain (MESQTQVLM SLLFVWSGTCG). Light- and heavy-chain sequences for this construct are given in Table 1. Signal peptides are shown in bold in Table 1. DNA constructs were transformed into *Escherichia coli* DH5 α cells for amplification under ampicillin selection and purified with a PureLink HiPure Plasmid Megaprep Kit (Invitrogen) according to the manufacturer’s instructions. Recombinant expression plasmids were then co-transfected at a 1:1 ratio into FreeStyle 293-F cells (Invitrogen) to allow expression of the recombinant antibody fragment.

The 293-F cells were cultured in FreeStyle expression medium (Invitrogen) and maintained at 37°C in an atmosphere of 8% CO₂. Expression was performed in 41 batches in a Certomat Ct plus incubator (Sartorius) by co-transfecting 1 \times 10⁶ cells ml⁻¹ with both DNA and 293Fectin transfection reagent (Invitrogen) according to the manufacturer’s instructions. Cultures were supplemented with 5 ml l⁻¹ 10% Pluronic F68 (Invitrogen), 5 mg l⁻¹ Lucratone Lupin (Millipore) 4 h post-transfection and with 5 mg l⁻¹ glucose 2 d post-transfection. The cell-culture supernatants were harvested by centrifugation at 500g and the media were collected for purification.

4 l of harvested media was concentrated to 200 ml by tangential flow filtration (Millipore Proflux M12). The concentrated media were centrifuged at 20 000g for 30 min before being purified by immobilized metal-affinity chromatography. The supernatant containing Fab was incubated for 1 h with Ni-NTA affinity resin (Qiagen) equilibrated in 20 mM Tris pH 8.0, 150 mM NaCl, 20 mM imidazole. The mixture was washed four times with 20 mM Tris pH 8.0, 150 mM NaCl, 20 mM imidazole. The protein of interest was eluted with 20 mM Tris pH 8.0, 150 mM NaCl, 500 mM imidazole. The eluted sample was further purified by size-exclusion chromatography (Fig. 1) with a HiLoad Superdex 200 20/60 run in PBS on an ÄKTApurifier (GE Healthcare). Fractions were concentrated to 2 mg ml⁻¹ with a centrifugal concentrator (Amicon Ultra, 10 kDa MWCO).

Protein-stabilizing buffers for crystallization were identified by a differential scanning fluorimetry (DFS) assay (Bio-Rad C1000 qPCR). For this study, the thermally induced melting points were determined in different buffers. 1 μ l SYPRO Orange dye

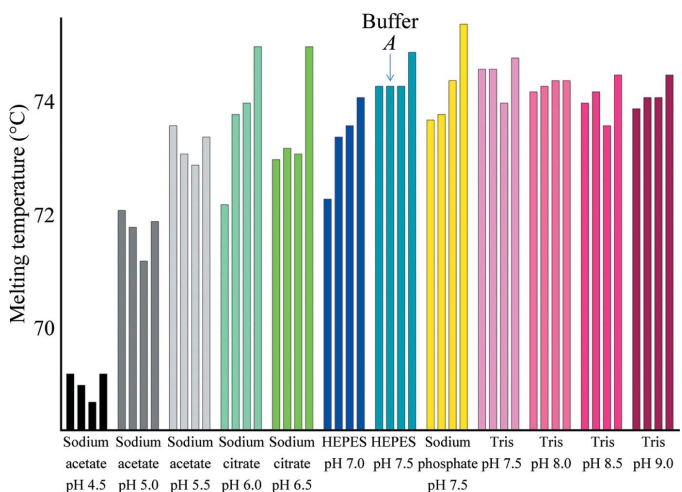


Figure 2
Melting points identified for the bapineuzumab Fab in different buffers. The four bars in each buffer represent (left to right) melting points at different concentrations of NaCl, namely 0, 50, 200 and 500 mM. Buffer A (20 mM HEPES pH 7.5, 50 mM NaCl) used as the Fab storage buffer is indicated by an arrow.

Table 2

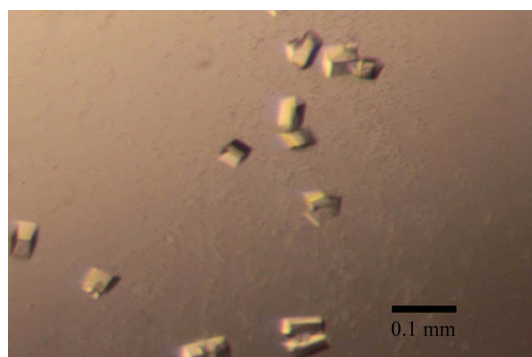
Data-collection statistics.

Data are from a single crystal. No outliers were observed in the Ramachandran plots.

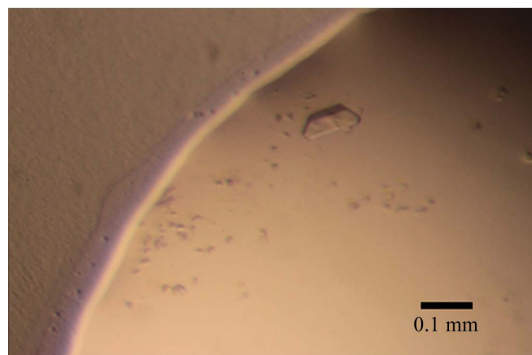
	Fab–A β_8	Fab–A β_{28}
Space group [†]	<i>P</i> 2 ₁ 2 ₂ 1	<i>P</i> 2 ₁ 2 ₂ 1
Unit-cell parameters (Å)	<i>a</i> = 60.2, <i>b</i> = 83.4, <i>c</i> = 88.3	<i>a</i> = 59.3, <i>b</i> = 83.0, <i>c</i> = 91.2
Resolution (Å)	2.0 (2.07–2.00)	2.2 (2.28–2.20)
Wavelength (Å)	0.9537	0.9537
No. of unique reflections	30725	22098
<i>R</i> _{merge} [‡] (%)	10.4 (36.9)	16.3 (78.8)
<i>R</i> _{p.i.m.} (%)	2.7 (9.9)	4.8 (34.3)
<i>R</i> _{r.i.m.} (%)	10.3 (38.2)	17.1 (84.7)
Mean <i>I</i> / σ (<i>I</i>)	23.4 (6.5)	11.2 (2.8)
Completeness (%)	100.0 (100.0)	94.4 (75.7)

[†] Data were indexed, refined and scaled in point group *P*222. Space groups were assigned after initial molecular replacement using *Phaser* from the *PHENIX* software suite (Adams *et al.*, 2010). [‡] $R_{\text{merge}} = \frac{\sum_{hkl} \sum_i |I_i(hkl) - \langle I(hkl) \rangle|}{\sum_{hkl} \sum_i I_i(hkl)}$, where $I_i(hkl)$ is the observed intensity and $\langle I(hkl) \rangle$ is the average intensity from multiple measurements.

(Invitrogen) was mixed with 250 μ l PBS buffer. Subsequently, 250 μ l diluted dye was combined with 250 μ l protein solution (0.5 mg ml⁻¹). Each screen contained 48 solutions in duplicate, sampling 0–500 mM NaCl and with a pH ranging from 4.5 to 9.0. 36 μ l of each buffer in the screen was combined with 4 μ l dye/protein mixture for DFS analysis (Fig. 2). Several buffers showed significant increases in protein melting temperature (T_m); the Fab showed a preference for the pH range 7.5–8.0 buffered with Tris or HEPES in all salt concentrations tested. Both buffers proved similarly stabilizing at high and low salt concentrations. We wanted some salt to be present to reduce nonspecific loss to surfaces during handling, but wanted a low salt concentration to aid handling during crystallization. Although we



(a)



(b)

Figure 3

Crystals of humanized 3D6–A β complexes. (a) Crystals of Fab–A β_8 . (b) Crystals of Fab–A β_{28} grown after seeding from crystals shown in (a).

chose HEPES pH 7.5, 50 mM NaCl as our storage buffer, Tris pH 7.5 or 8.0, 50 mM NaCl would likely have served just as well. Protein samples were extensively dialysed against buffer *A* (20 mM HEPES pH 7.5, 50 mM NaCl) which gave a Fab melting point of 74.5°C. The protein was concentrated to 5 mg ml⁻¹ and stored in small aliquots at –80°C until required for crystallization.

Peptides corresponding to residues 1–8 (A β_8) and 1–28 (A β_{28}) of the wild-type amyloid- β sequence (DAEFRHDSGYEVHHQ-KLVFFAEDVGSNKGAIIGLMVGGVVIA) were obtained from GenicBio and AnaSpec, respectively. These were resuspended in neat trifluoroethanol (TFE, Sigma) and aliquoted to give 100 μ g per Eppendorf tube. All aliquots were freeze-dried for 4 h and stored at –80°C until required.

2.2. Crystallization

TFE-treated and thoroughly lyophilized peptides were taken up in 5 μ l 10 mM NaOH, diluted twofold with buffer *A* to a final concentration of 100 mg ml⁻¹ and quickly added to the Fab sample to a Fab:A β molar ratio of 1:5. Excess A β was not removed prior to crystallization.

To confirm the complex formation of Fab produced in-house with the two A β peptides, the complexes were separated by size-exclusion chromatography and analysed by mass spectrometry on an Agilent 6510 Q-TOF LC/MS (Bio21 Institute, University of Melbourne). MS/MS confirmed that the protein binds to the A β peptide. The initial crystallization screening for Fab–A β_8 and Fab–A β_{28} was performed in-house using The PEGs Suite screen (Qiagen). All crystals were grown in 2 μ l hanging drops (1 μ l sample solution, 1 μ l reservoir solution) at 25°C equilibrated with 0.5 ml reservoir solution.

The first well diffracting crystals were comprised of the Fab–A β_8 complex and were obtained from 0.1 M HEPES pH 7.5, 25% (w/v) PEG 6000 (Fig. 3a). In case the complete recognition epitope of A β extended beyond residue 8 or more than the epitope could be visualized by crystallography, these Fab–A β_8 crystals were used to promote crystallization of the Fab–A β_{28} complex *via* microseed matrix screening (MMS; Obmolova *et al.*, 2010). Fab–A β_8 crystals used for seed-stock preparation were placed in 100 μ l reservoir solution, homogenized by vortex mechanical agitation for 3 min with a Teflon Seed Bead (Hampton Research) and stored at –20°C. The MMS for Fab–A β_{28} was set up manually with The PEGs Suite using the hanging-drop vapour-diffusion method in 24-well greased plates (Hampton Research). In each crystallization drop, 0.6 μ l screening (reservoir) solution and 0.2 μ l microseeds were added to 0.8 μ l protein solution. The protein droplets were equilibrated over 500 μ l reservoir solution. The best crystals obtained for the Fab–A β_{28} complex were grown with reservoir solution consisting of 0.2 M sodium formate, 20% (w/v) PEG 3350 (Fig. 3b). The space group was the same as for the seeding crystals, *P*2₁2₂1, but the unit-cell volume was slightly smaller (*a* = 59.3, *b* = 83.0, *c* = 91.2 Å compared with *a* = 60.2, *b* = 83.4, *c* = 88.3 Å).

Crystals of both complexes were harvested after 2 d. The crystals were soaked for 1 min in a cryoprotectant [10% (v/v) glycerol and reservoir solution], cryocooled in liquid nitrogen and mounted in a cryostream at –173°C for data collection.

2.3. Data collection and preliminary X-ray analysis

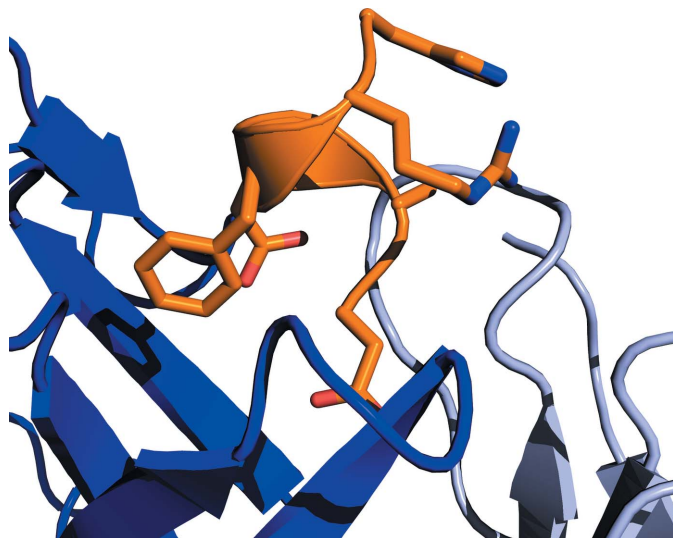
Complete X-ray diffraction data sets were collected from single crystals obtained by co-crystallization of Fab and A β peptides. The data were collected on the microfocus MX2 beamline at the Australian Synchrotron, Clayton, Victoria. For each crystal described in Table 2, images were obtained at a single wavelength of 0.9537 Å in

Table 3Data-refinement statistics for the Fab–A β_8 complex.

Space group	$P2_122_1$
Resolution (Å)	2.0
No. of reflections	30725
$R_{\text{work}}/R_{\text{free}}$ (%)	17.2/21.5
No. of atoms	
Total	3680
Protein	3324
Ligand/ion	54
Water	302
B factors (Å ²)	
Protein	27.6
Ligand/ion	19.8
Water	31.2
R.m.s. deviations	
Bond lengths (Å)	0.008
Bond angles (°)	1.210

a nitrogen cryostream (−173°C). 720 images were acquired with 0.5° oscillations about φ over 360°. The data collection was controlled using the *Blu-Ice* software (McPhillips *et al.*, 2002).

The data were indexed, integrated and scaled using the *HKL-2000* software package (Otwinowski & Minor, 1997). The best crystal for Fab–A β_{28} diffracted to a resolution of 2.2 Å and belonged to the primitive orthorhombic space group $P2_122_1$, with refined unit-cell parameters $a = 59.3$, $b = 83.0$, $c = 91.2$ Å. The high-resolution three-dimensional structure of Fab–A β_{28} based on these data has been described in detail elsewhere (Miles *et al.*, 2013) and coordinates have been deposited in the Protein Data Bank under accession code 4hix. We subsequently obtained improved diffraction from a Fab–A β_8 crystal to 2.0 Å resolution in the same space group and with unit-cell parameters $a = 60.2$, $b = 83.4$, $c = 88.3$ Å. The resultant structure has been deposited in the PDB under accession code 4ojf. Data-collection statistics are shown in Table 2 and data-refinement statistics are shown in Table 3. The high-resolution three-dimensional structure of Fab–A β_8 based on these data proved to be identical to the published Fab–A β_{28} complex structure with only residues 1–5 visible in the

**Figure 4**

Structure of humanized 3D6–A β_8 showing the helical N-terminal structure of A β (orange) in the 3D6 Fab binding pocket formed at the interface of the heavy chain (dark blue) and light chain (light blue).

electron-density map (Fig. 4). Interestingly, the R_{merge} value for Fab–A β_8 is substantially better than for the Fab–A β_{28} crystal, perhaps as a consequence of removing 20 of the disordered 23 amino acids of A β_{28} . The antibody was found to recognize both peptides in a helical rather than a linear conformation (Miles *et al.*, 2103).

We would like to thank Aidan Williams at Emmanuel College for his contribution to validating Fab binding to A β . This research was partly undertaken on the MX1 and MX2 beamlines at the Australian Synchrotron, Victoria, Australia. This work was supported by funding from a National Health and Medical Research Council of Australia (NHMRC) Project Grant (APP1021935) and grants from the JO & JR Wicking Trust, The Mason Foundation and The Bethlehem Griffith Research Foundation to MWP and LAM. The Australian Cancer Research Foundation provided substantial funding support for equipment critical for this work. Infrastructure support from the NHMRC Independent Research Institutes Infrastructure Support Scheme and the Victorian State Government Operational Infrastructure Support Program are gratefully acknowledged. DBA was supported by a Victoria Fellowship from the Victorian Government and the Leslie (Les) J. Fleming Churchill Fellowship from The Winston Churchill Memorial Trust. MWP is an NHMRC Research Fellow.

References

- Adams, P. D. *et al.* (2010). *Acta Cryst.* **D66**, 213–221.
- Blennow, K., Zetterberg, H., Rinne, J. O., Salloway, S., Wei, J., Black, R., Grundman, M. & Liu, E. (2012). *Arch. Neurol.* **69**, 1002–1010.
- Chen, G., Chen, K. S., Kobayashi, D., Barbour, R., Motter, R., Games, D., Martin, S. J. & Morris, R. G. (2007). *J. Neurosci.* **27**, 2654–2662.
- Gilman, S., Koller, M., Black, R. S., Jenkins, L., Griffith, S. G., Fox, N. C., Eisner, L., Kirby, L., Rovira, M. B., Forette, F. & Orgogozo, J. M. (2005). *Neurology*, **64**, 1553–1562.
- Johnson-Wood, K., Lee, M., Motter, R., Hu, K., Gordon, G., Barbour, R., Khan, K., Gordon, M., Tan, H., Games, D., Lieberburg, I., Schenk, D., Seubert, P. & McConlogue, L. (1997). *Proc. Natl Acad. Sci. USA*, **94**, 1550–1555.
- Masters, C. L., Simms, G., Weinman, N. A., Multhaup, G., McDonald, B. L. & Beyreuther, K. (1985). *Proc. Natl Acad. Sci. USA*, **82**, 4245–4249.
- McPhillips, T. M., McPhillips, S. E., Chiu, H.-J., Cohen, A. E., Deacon, A. M., Ellis, P. J., Garman, E., Gonzalez, A., Sauter, N. K., Phizackerley, R. P., Soltis, S. M. & Kuhn, P. (2002). *J. Synchrotron Rad.* **9**, 401–406.
- Miles, L. A., Crespi, G. A., Doughty, L. & Parker, M. W. (2013). *Sci. Rep.* **3**, 1302.
- Miles, L. A., Wun, K. S., Crespi, G. A. N., Fodero-Tavoletti, M. T., Galatis, D., Bagley, C. J., Beyreuther, K., Masters, C. L., Cappai, R., McKinstry, W. J., Barnham, K. J. & Parker, M. W. (2008). *J. Mol. Biol.* **377**, 181–192.
- Moreth, J., Mavoungou, C. & Schindowski, K. (2013). *Immun. Ageing*, **10**, 18–26.
- Obmolova, G., Malia, T. J., Teplyakov, A., Sweet, R. & Gilliland, G. L. (2010). *Acta Cryst.* **D66**, 927–933.
- Orgogozo, J. M., Gilman, S., Dartigues, J. F., Laurent, B., Puel, M., Kirby, L. C., Jouanny, P., Dubois, B., Eisner, L., Flitman, S., Michel, B. F., Boada, M., Frank, A. & Hock, C. (2003). *Neurology*, **61**, 46–54.
- Otwinowski, Z. & Minor, W. (1997). *Methods Enzymol.* **276**, 307–326.
- Prince, M., Prina, M. & Guerchet, M. (2013). *World Alzheimer Report 2013*. London: Alzheimer's Disease International.
- Rinne, J. O. *et al.* (2010). *Lancet Neurol.* **9**, 363–372.
- Schroeter, S. & Games, K. D. (2008). US Patent Application 20080292625.
- Selkoe, D. J. (1999). *Nature (London)*, **399**, A23–A31.
- Selkoe, D. J. (2012). *Science*, **337**, 1488–1492.
- Tabaton, M. & Tamagno, E. (2007). *Cell. Mol. Life Sci.* **64**, 2211–2218.
- Wun, K. S., Miles, L. A., Crespi, G. A. N., Wycherley, K., Ascher, D. B., Barnham, K. J., Cappai, R., Beyreuther, K., Masters, C. L., Parker, M. W. & McKinstry, W. J. (2008). *Acta Cryst.* **F64**, 438–441.